Source-detector trajectory optimization for FOV extension in dental CBCT imaging: Supplementary Materials

S M Ragib Shahriar Islam[a,b,c], Ander Biguri[d], Claudio Landi[e], Giovanni Di Domenico[f], Benedikt Schneider[g], Pascal Grün[g], Cristina Sarti[e], Ramona Woitek[b], Andrea Delmiglio[e], Carola-Bibiane Schönlieb[d], Dritan Turhani[g], Gernot Kronreif[a], Wolfgang Birkfellner[c], Sepideh Hatamikia[b,a]

[a]*Austrian Center for Medical Innovation and Technology, Wiener Neustadt, Austria*
[b]*Department of Medicine, Danube Private University, Krems, Austria*
[c]*Center for Medical Physics and Biomedical Engineering, Medical University Vienna, Vienna, Austria*
[d]*Department of Applied Mathematics and Theoretical Physics, University of Cambridge, Cambridge, United Kingdom*
[e]*SeeThrough SrL, Via Bolgara 2, Brusaporto (BG), Italy*
[f]*Department of Physics and Earth Science, University of Ferrara, Ferrara, Italy*
[g]*Center for Oral and Maxillofacial Surgery, Department of Dentistry, Faculty of Medicine and Dentistry, Danube Private University, Steiner Landstraße 124, Krems, 3500, Austria*

Appendix A. Search space for the valid and invalid region of the trajectory

There is a 11cm × 6cm rectangular space where the iso-center can be dynamically placed during the scan. Therefore, considering the circular trajectory, for every possible iso-center location, there is a certain valid and invalid limited angular portion of the trajectory. In Figure A.1 (A), (B), (C), (D), (E), the iso-center is placed at the middle, extreme left-front, extreme right-front, extreme left-back, and extreme right-back positions respectively, and delineates the valid (black line) and non-valid (red line) portion of the circular trajectory. Figure A.1 (F) shows the valid and invalid portions for all the extreme points. Similarly, the iso-center location is considered at 1cm, and all the possible valid and invalid portion is calculated as Figure

A.1 (G). The combination of all these projection angles for valid and non-valid portions of the circular trajectory at every possible iso-center location is considered as the search space for the proposed trajectory.

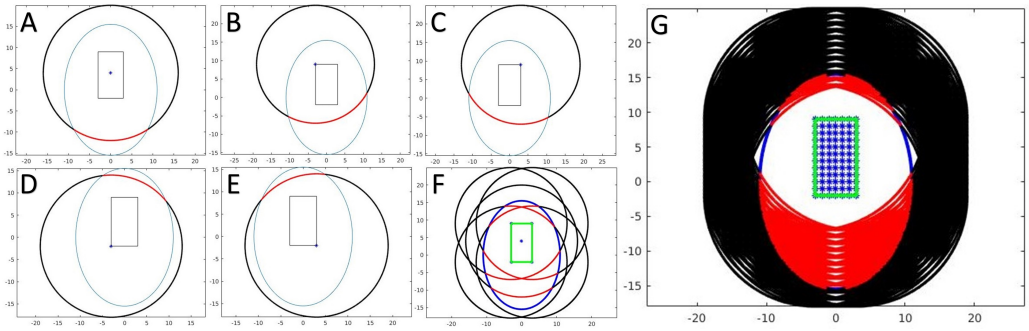

Figure A.1: The limited angle circular trajectory when the iso-center is at **A:** the centroid, **B:** Up-Left, **C:** Up-Right, **D:** Down-Left, and **E:** Down-Right of the possible iso-center moving region. Illustration of the possible detector movement space and collision area considering **F:** iso-centers at Figure A, B, C, D, E together and **G:** iso-centers at all the possible position at $1cm$ apart in the rectangle region.

Appendix B. The Peak Signal to Noise Ratio (PSNR)

PSNR is one of the most widely used image quality metrics to evaluate the signal fidelity of a reconstructed image compared to the ground truth image. PSNR does not directly measure the visual quality of an image, rather it measures the similarity of the signal fidelity between two images. However, the visual quality and the measurement of signal fidelity are highly correlated. The PSNR value of more than 30dB is considered as good image reconstruction fidelity [1]. The expression of the PSNR is based on the Mean Squared Error (MSE) as follows,

$$MSE = \frac{1}{m \times n \times p} \sum_{i=1}^{m} \sum_{j=1}^{n} \sum_{k=1}^{p} [V(i,j,k) - \widehat{V}(i,j,k)]^2 \qquad \text{(B.1)}$$

where V is the ground truth image and $\widehat{V}$ is the reconstructed image. $m \times n \times p$ and i, j, k are the volume size and voxel values respectively.
From the MSE value, the PSNR is calculated in dB as follows where the

MAX is the maximum possible value of a voxel.

$$PSNR = 10 \cdot \log_{10} \left(\frac{MAX^2}{MSE} \right) \tag{B.2}$$

Appendix C. Structural Similarity Index Measurements (SSIM)

SSIM measures the quality of an image in terms of the visual appearance of the image. It measures the similarity between two images in terms of the luminance, contrast, and structure of the image ([2]). The mathematical model of SSIM is defined as

$$SSIM(V, \widehat{V}) = \frac{(2\mu_V \mu_{\widehat{V}} + c_1)(2\sigma_{V\widehat{V}} + c_2)}{(\mu_V^2 + \mu_{\widehat{V}}^2 + c_1)(\sigma_V^2 + \sigma_{\widehat{V}}^2 + c_2)} \tag{C.1}$$

where μ_V and $\mu_{\widehat{V}}$ are the average voxel value of image V and $\widehat{V}$, respectively. $\sigma_{V\widehat{V}}$ represents the covariance between the two images. And σ_V^2 and $\sigma_{\widehat{V}}^2$ is the variances of voxels values of image V and $\widehat{V}$, respectively. c_1 and c_2 are two constant values that stabilize the division if the mean, variance, or covariance elements get tend to zero. By measuring "μ_V and $\mu_{\widehat{V}}$", "σ_V^2 and $\sigma_{\widehat{V}}^2$", and "$\sigma_{V\widehat{V}}$" SSIM measures and compares "luminance", "contrast", and "structure similarity" between the images V and $\widehat{V}$ respectively. The range of the SSIM metric is between 0 and 1. The closer the SSIM value to 1, indicates the better the image quality to be [1, 2].

Appendix D. Universal Quality Index (UQI):

UQI is another widely used metric which also measure the visual appearance of the reconstructed image in therms of the luminance, contrast, and structural information [3]. The mathematical expression of UQI is as follows,

$$UQI = \frac{2\sigma_{V\widehat{V}}}{\sigma_V^2 \sigma_{\widehat{V}}^2} \cdot \frac{2\mu_V \mu_{\widehat{V}}}{\mu_V^2 + \mu_{\widehat{V}}^2} \tag{D.1}$$

where, $\sigma_{V\widehat{V}}$, $\sigma_{V,\widehat{V}}^2$, and $\mu_{V,\widehat{V}}$ are the covariance, variances, and means of the voxel values respectively for the images V and $\widehat{V}$. The UQI measurement has been added as it also measures the visual quality of the image as SSIM, however, in a different way. Therefore, the SSIM and UQI values can be cross-checked to support each other. The UQI also ranges from 0 to 1 as same as the SSIM measurement, closer the value to 1 indicates the better image quality.

Appendix E. Root Mean Squared Error (RMSE)

The RMSE is one of the fundamental and most widely used metrics for measuring predicted and actual data. In the case of image reconstruction, it is calculated as the square root of the mean of the squared differences between the corresponding voxels of the two images. The expression of the RMSE is as follows.

$$RMSE(V, \widehat{V}) = \sqrt{\frac{1}{m \times n \times p} \sum_{i=1}^{m} \sum_{j=1}^{m} \sum_{k=1}^{p} [V(i,j,k) - \widehat{V}(i,j,k)]^2} \qquad \text{(E.1)}$$

The range of RMSE depends on the range of voxel values. For our study, all the images were normalized in the range of 0 and 1. Therefore, the RMSE range is also limited to the same range. However, as RMSE is residual voxel-to-voxel error measurement, closer the value to 0, indicates better image quality as it refers to the minimal error.

Appendix F. Extended quantitative measurement of reconstructed images

Trajectory	VOI	PSNR		SSIM		UQI		RMSE	
		In VOI	Whole slice	in VOI	Whole slice	in VOI	Whole slice	in VOI	Whole slice
Circular; OSSART	Sinus	28.5935	21.1281	0.9792	0.7520	0.8921	0.8755	0.0372	0.0878
	TMJ	37.4164	22.1337	0.9935	0.7789	0.9599	0.8929	0.0135	0.0782
	Upper Jaw	25.7520	22.7246	0.9542	0.8170	0.9274	0.9164	0.0516	0.0731
	Lower Jaw	27.4749	25.0951	0.9672	0.8597	0.9467	0.9453	0.0423	0.0556
	Chin	31.1546	27.0987	0.9834	0.9080	0.9505	0.9500	0.0277	0.0442
Fusion; OSSART	Sinus	36.1103	30.7057	0.9837	0.8686	0.9873	0.9877	0.0156	0.0292
	TMJ	43.2929	31.1151	0.9948	0.8672	0.9895	0.9875	0.0068	0.0278
	Upper Jaw	32.6921	30.8363	0.9598	0.8996	0.9884	0.9878	0.0232	0.0287
	Lower Jaw	33.4874	31.3960	0.9691	0.9084	0.9891	0.9884	0.0212	0.0269
	Chin	35.1400	32.1087	0.9816	0.9148	0.9860	0.9870	0.0175	0.0248
Fusion; ASDPOCS	Sinus	46.6413	40.1683	0.9962	0.9665	0.9991	0.9987	0.0047	0.0098
	TMJ	53.8594	41.5986	0.9991	0.9688	0.9993	0.9990	0.0020	0.0083
	Upper Jaw	45.0462	42.8082	0.9946	0.9832	0.9994	0.9993	0.0056	0.0072
	Lower Jaw	45.7294	43.3618	0.9962	0.9860	0.9995	0.9994	0.0052	0.0068
	Chin	49.0815	45.7565	0.9986	0.9912	0.9995	0.9995	0.0035	0.0052
Fusion; OSSART; Reduced projections	Sinus	35.1702	30.3879	0.9829	0.8696	0.9851	0.9869	0.0174	0.0302
	TMJ	43.2229	30.9937	0.9950	0.8743	0.9896	0.9871	0.0069	0.0282
	Upper Jaw	32.1469	30.4541	0.9609	0.9027	0.9874	0.9869	0.0247	0.0300
	Lower Jaw	33.0697	31.1404	0.9704	0.9140	0.9885	0.9879	0.0222	0.0277
	Chin	34.3213	31.6757	0.9831	0.9245	0.9838	0.9858	0.0192	0.0261
Fusion; ASDPOCS; Reduced projections	Sinus	41.1827	35.3547	0.9941	0.9499	0.9963	0.9959	0.0087	0.0171
	TMJ	49.0731	36.6566	0.9987	0.9573	0.9975	0.9967	0.0035	0.0147
	Upper Jaw	38.9620	36.9718	0.9923	0.9716	0.9974	0.9972	0.0113	0.0142
	Lower Jaw	39.5378	37.5330	0.9945	0.9765	0.9974	0.9973	0.0105	0.0133
	Chin	41.5771	38.5493	0.9977	0.9856	0.9967	0.9971	0.0083	0.0118

Table F.1: Jerry: Quality measurement scores in different VOIs for different trajectories and corresponding reconstruction algorithms. Measurement is taken at the most prominent slices of the respected VOI along the z-axis. **In VOI:** measurement only inside each VOI region; **Whole Slice:** measurement in the whole slice related to each VOI.

Trajectory	PSNR		SSIM		UQI		RMSE	
	(in VOI)	(Whole Volume)	(in VOI)	(Whole Volume)	(in VOI)	(Whole Volume)	(in VOI)	(Whole Volume)
Circular;OSSART	31.8048	25.9080	0.9880	0.9373	0.9342	0.9160	0.0257	0.0507
Fusion;OSSART	38.2879	33.3871	0.9896	0.9444	0.9886	0.9879	0.0122	0.0214
Fusion;ASDPOCS	50.3861	45.0632	0.9986	0.9917	0.9994	0.9993	0.0030	0.0056
Fusion;OSSART; Reduced projections	37.7906	33.1499	0.9899	0.9491	0.9878	0.9875	0.0129	0.0220
Fusion;ASDPOCS; Reduced projections	44.2543	38.6958	0.9979	0.9885	0.9972	0.9967	0.0061	0.0116

Table F.2: Jerry: Quality measurement scores measured in the whole reconstructed volume for different trajectories and corresponding reconstruction algorithms. **In VOI:** measurement in the total VOI region (related to all five VOIs); **Whole Volume:** measurement in the whole reconstructed volume containing the VOI.

Trajectory	VOI	PSNR		SSIM		UQI		RMSE	
		(in VOI)	(Whole slice)	(in VOI)	(Whole slice)	(in VOI)	(Whole slice)	(in VOI)	(Whole slice)
Circular; OSSART	Sinus	24.8817	15.5644	0.9567	0.6810	0.1520	0.0927	0.0570	0.1666
	TMJ	31.8350	15.7035	0.9892	0.6824	0.1599	0.0903	0.0256	0.1640
	Upper Jaw	20.8897	15.8851	0.9354	0.7131	0.0824	0.0830	0.0903	0.1606
	Lower Jaw	21.4372	16.3203	0.9432	0.7202	0.1108	0.0962	0.0848	0.1528
	Chin	23.4239	17.2051	0.9630	0.7802	0.1068	0.1059	0.0674	0.1380
Fusion; OSSART	Sinus	38.7543	29.7584	0.9912	0.9164	0.9798	0.9726	0.0115	0.0325
	TMJ	45.7258	30.3802	0.9985	0.9158	0.9798	0.9755	0.0052	0.0303
	Upper Jaw	34.9699	31.0197	0.9876	0.9233	0.9788	0.9786	0.0178	0.0281
	Lower Jaw	35.5231	31.7132	0.9908	0.9303	0.9795	0.9803	0.0167	0.0260
	Chin	39.3963	33.9972	0.9960	0.9568	0.9853	0.9858	0.0107	0.0200
Fusion; ASDPOCS	Sinus	47.8494	35.2701	0.9976	0.9599	0.9975	0.9932	0.0041	0.0172
	TMJ	53.1047	34.8657	0.9997	0.9592	0.9967	0.9922	0.0022	0.0181
	Upper Jaw	45.2907	37.6667	0.9977	0.9641	0.9979	0.9958	0.0054	0.0131
	Lower Jaw	45.8654	39.1038	0.9989	0.9703	0.9980	0.9968	0.0051	0.0111
	Chin	48.4115	40.2593	0.9993	0.9770	0.9981	0.9970	0.0038	0.0097
Fusion; OSSART; Reduced projections	Sinus	40.3104	31.2519	0.9909	0.9085	0.9899	0.9842	0.0096	0.0274
	TMJ	47.1235	30.7181	0.9984	0.9047	0.9901	0.9813	0.0044	0.0291
	Upper Jaw	36.5774	31.3960	0.9885	0.9083	0.9893	0.9840	0.0148	0.0269
	Lower Jaw	37.1682	33.0961	0.9909	0.9284	0.9901	0.9889	0.0139	0.0221
	Chin	42.7239	36.6161	0.9963	0.9524	0.9957	0.9944	0.0073	0.0148
Fusion; ASDPOCS; Reduced projections	Sinus	40.2724	31.3741	0.9919	0.9195	0.9896	0.9841	0.0097	0.0270
	TMJ	46.5171	31.1403	0.9980	0.9240	0.9883	0.9824	0.0047	0.0277
	Upper Jaw	37.3895	31.7105	0.9908	0.9313	0.9907	0.9844	0.0135	0.0260
	Lower Jaw	38.1525	33.8002	0.9924	0.9488	0.9919	0.9902	0.0124	0.0204
	Chin	42.7103	36.5687	0.9966	0.9621	0.9954	0.9941	0.0073	0.0148

Table F.3: Tom: Quality measurement scores in different VOIs for different trajectories and corresponding reconstruction algorithms. Measurement is taken at the most prominent slices of the respected VOI along the z-axis. **In VOI:** measurement only inside each VOI region; **Whole Slice:** measurement in the whole slice related to each VOI.

Trajectory	PSNR		SSIM		UQI		RMSE	
	(in VOI)	(Whole Volume)	(in VOI)	(Whole Volume)	(in VOI)	(Whole Volume)	(in VOI)	(Whole Volume)
Circular;OSSART	27.8173	21.3781	0.9826	0.9075	0.0989	0.0904	0.0407	0.0853
Fusion;OSSART	42.4092	36.7414	0.9978	0.9805	0.9814	0.9817	0.0076	0.0145
Fusion;ASDPOCS	51.9708	42.8008	0.9996	0.9910	0.9978	0.9961	0.0025	0.0072
Fusion;OSSART; Reduced projections	44.2972	37.5982	0.9980	0.9777	0.9917	0.9897	0.0061	0.0132
Fusion;ASDPOCS; Reduced projections	44.6559	37.6372	0.9981	0.9819	0.9921	0.9891	0.0059	0.0131

Table F.4: Tom: Quality measurement scores measured in the whole reconstructed volume for different trajectories and corresponding reconstruction algorithms. **In VOI:** measurement in the total VOI region (related to all five VOIs); **Whole Volume:** measurement in the whole reconstructed volume containing the VOI.

Appendix G. Detailed FOV measurements

Trajectory	Sinus		TMJ		Upper Jaw		Lower Jaw		Chin	
	Cran.	N.O.	Cran.	N.O.	Cran.	N.O.	Cran.	N.O.	Cran.	N.O.
Circular; OSSART	11cm	11cm	11cm	11cm	11cm	11cm	11cm	11cm	11cm	11cm
Fusion; OSSART	14cm	16.5cm	14cm	16.5cm	14cm	15.5cm	14cm	15.5cm	11cm	15.5cm
Fusion; ASDPOCS	14cm	16.5cm	14cm	16.5cm	14cm	15.5cm	14cm	15.5cm	11cm	15.5cm

Table G.5: Jerry: The measured FOV in the axial axis of different VOIs containing slices from the reconstructed images using different trajectories. (Cran.: In Cranial breadth; N.O: In Naso-occipital length)

Trajectory	Sinus		TMJ		Upper Jaw		Lower Jaw		Chin	
	Cran.	N.O.	Cran.	N.O.	Cran.	N.O.	Cran.	N.O.	Cran.	N.O.
Circular; OSSART	11cm	11cm	11cm	11cm	11cm	11cm	11cm	11cm	11cm	11cm
Fusion; OSSART	15cm	19.5cm	15cm	19.5cm	15cm	18.5cm	15cm	18.5cm	12.5cm	18.5cm
Fusion; ASDPOCS	15cm	19.5cm	15cm	19.5cm	15cm	18.5cm	15cm	18.5cm	12.5cm	18.5cm

Table G.6: Tom: The measured FOV in the axial axis of different VOIs containing slices from the reconstructed images using different trajectories.(Cran.: In Cranial breadth; N.O: In Naso-occipital length)

Appendix H. Image quality measurement score characteristics for different trajectory and reconstruction techniques

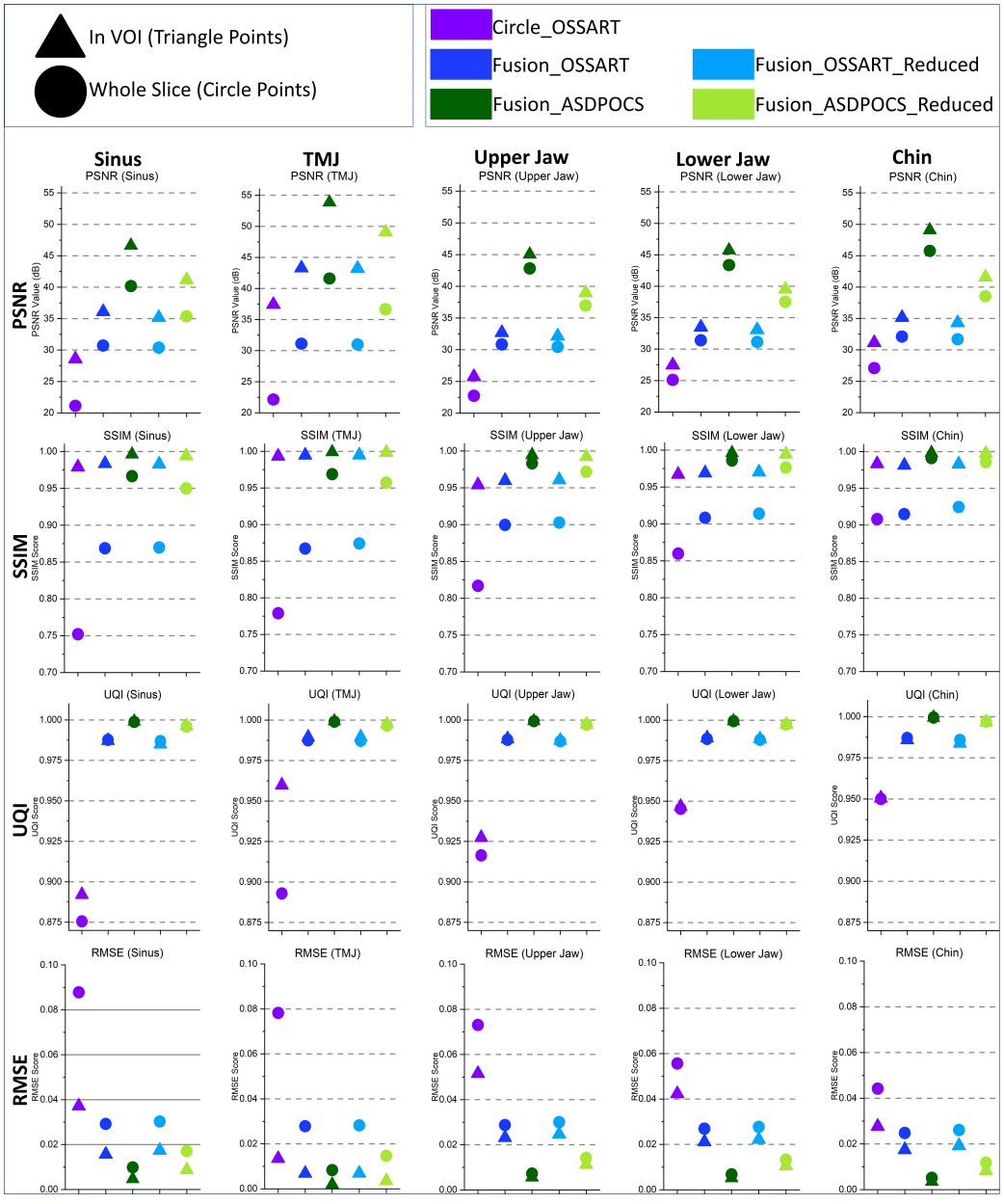

Figure H.2: Image quality measurement score characteristics in Jerry

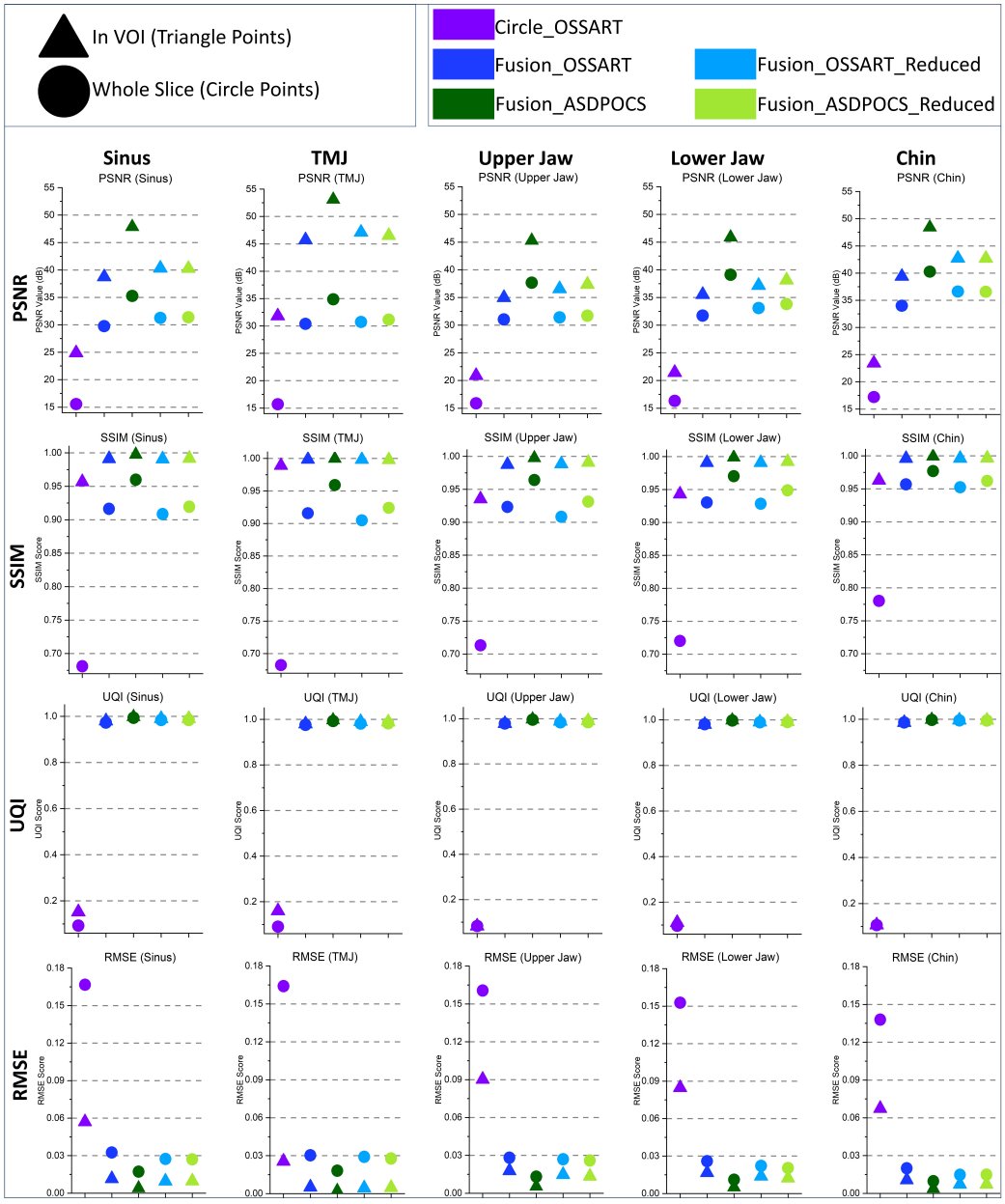

Figure H.3: Image quality measurement score characteristics in Tom

References

[1] A. Hore, D. Ziou, Image quality metrics: PSNR vs. SSIM, in: 2010 20th international conference on pattern recognition, IEEE, 2010, pp. 2366–

2369.

[2] Z. Wang, A. C. Bovik, H. R. Sheikh, E. P. Simoncelli, Image quality assessment: from error visibility to structural similarity, IEEE transactions on image processing 13 (4) (2004) 600–612.

[3] Z. Wang, A. C. Bovik, A universal image quality index, IEEE signal processing letters 9 (3) (2002) 81–84.